

Deformation Behavior of Polystyrene as a Function of Molecular Weight Parameters

JOHN F. FELLERS and THEODORE F. CHAPMAN,* *Department of Chemical and Metallurgical Engineering, The University of Tennessee, Knoxville, Tennessee 37916*

Synopsis

The mechanical deformation of polystyrene as it relates to molecular weight parameters was investigated. Mechanical testing consisted of uniaxial tension and compression experiments on a variety of polystyrenes. Such quantities as modulus, proportional limit, and various yield stress measurements were determined on polystyrene samples of controlled number-average molecular weight and molecular weight distribution. A basic tool for the mechanical behavior analysis was the use of a power law equation $\sigma = K\epsilon^n$ to examine the initial nonlinear region of each experimentally determined stress-strain curve. Correlations between mechanical deformation and molecular weight parameters were determined using statistical linear regression analysis. It was generally found for uniaxial tension that mechanical parameters in or near the elastic region were independent of \bar{M}_n and MWD, while at larger strains correlations were found. For uniaxial compression, stress maxima and the strain where this occurred increased with increasing MWD. Otherwise, mechanical parameter changes in uniaxial compression did not occur with changing \bar{M}_n and MWD. Finally, a direct comparison of tension versus compression showed only the initial moduli to be the same. All other mechanical parameters showed significantly differing values, indicating different deformation mechanisms operating in tension versus compression. The analysis of this behavior from both a mechanics and molecular weight viewpoint provides some insight about glassy polymer deformation processes on the microscopic level.

INTRODUCTION

The deforming of a rigid glassy polymer may be viewed as a process influenced by many factors. Studies directed toward the phenomenological description of the process have shown rather complex interrelationships among the controlling factors. Strain rate,¹⁻³ test temperature along with its relation to T_g ,⁴ the applied stress field with cognizance of hydrostatic pressure effects,⁵ and also molecular level features⁶⁻⁸ play interacting roles in glassy polymer deformation.

The effect of the applied stress field has recently been under scrutiny. This line of research has been fruitful. It is now understood that crazing occurs only when the tensile component of the applied stress field exceeds a critical value.⁹ Also another type of heterogeneous microdeformation, shear banding, occurs as the nature of the stress field changes. This was observed when a hydrostatic pressure was imposed on a sample tested in uniaxial tension. This study led to the important insight that the brittle-to-ductile transition is controlled by the change from crazing to a shear banding mechanism.^{10,11} Much work on stress field considerations was motivated by the important observation that slight volume changes occur during the deformation process.⁵ Furthermore, this ob-

* Present address: B. F. Goodrich Chemical Co., Technical Center, Avon Lake, Ohio 44012.

servation has caused some rethinking about the anisotropy of the yield surface and other mechanical features of rigid amorphous polymers.

In addition to the mechanics of glassy polymer systems, some consideration has also been given to the role of molecular level features in glassy polymer deformation. These features have been explored enough to suggest their significance, but not enough to provide clear insight. For example, the effect of chemical structure can be appreciated when one compares polystyrene (PS), poly(methyl methacrylate) (PMMA), and polycarbonate (PC) in tension. Crazing is common to all three and acts as a precursor to failure in the tensile mode, yet at certain equivalent ($T_g - T$) test temperatures PS can be brittle while PMMA would show limited ductility and PC would be ductile and tough. The most apparent difference among the three is chemical structure and is thought to be playing a role, but definitive explanation in quantitative fundamental concepts is still awaited.

Molecular weight is another feature of interest. Several papers^{8,12-14} present evidence that strength, crazing, and mechanical properties in general⁶ respond to MW and MWD. However, the effort to more fully develop this aspect has been hampered by the paucity of studies where quantitative evaluation of both mechanical and molecular weight characteristics were pursued. In the present paper we strive to do both in the study of PS deformation.

EXPERIMENTAL TECHNIQUES AND RESULTS

Polystyrene

The polystyrenes used in this study were either synthesized via anionic polymerization or were commercially available. The anionic polymerization was accomplished using high vacuum techniques, with butyllithium initiator, and a benzene solvent system containing 10% triethylamine to ensure a high rate of initiation compared to the propagation rate. This enabled polystyrene to be made in a range of molecular weights with a $MWD \leq 1.2$. This study was also concerned with the influence of MWD on mechanical properties. Thus, in addition to the near-monodisperse samples and the commercial polystyrene, two solution-blended mixtures were made to give MWDs in the range of 6.

All polystyrenes used were characterized via gel permeation chromatography (GPC) with a Waters Associates Model 200 GPC. It was calibrated using several monodisperse polystyrenes of known \bar{M}_n available from Waters Associates. A complete list of the molecular weight characteristics of all polystyrenes used in the deformation study is given in Table I.

Samples for Mechanical Testing

Tensile bars were nominally ASTM D638 (Type 1), formed directly by compression molding and then annealing. Surface treatment of these bars involved various levels of sanding to remove all surface flaws and finishing with 600 grit metallurgical paper. All sanding was done in the direction parallel to the gauge length. By using this technique, i.e., 600 grit paper as the final step and only stroking in the loading direction, load-deformation curves were obtained that showed a loading maximum.

Samples for compression testing were also fabricated by compression molding.

TABLE I
Molecular Weight Characteristics of Polystyrenes Investigated

Polymer	$\bar{M}_w \times 10^{-4}$	$\bar{M}_n \times 10^{-4}$	\bar{M}_w/\bar{M}_n
1	6.00	4.99	1.20
2	12.8	11.1	1.15
3	20.2	17.3	1.17
4	23.0	20.2	1.14
5 ^a	26.3	24.7	1.06
6	40.2	36.7	1.09
7	128	108	1.19
8	151	123	1.23
9	25.0	11.1	2.25
(Monsanto HHI-101)			
10	33.9	11.4	2.97
(U.S. Steel)			
Bimodal Mixture			
1 (19.7 g)	71.4	11.1	6.43
7 (40.3 g)			
Tetramodal Mixture			
1 (14.1 g)	71.7	11.1	6.46
7 (10.1 g)			
8 (20.3 g)			
10 (15.5 g)			

^a Courtesy of Dr. L. H. Tung, The Dow Research Lab, Midland, Michigan.

The test piece was a tetragonal specimen of nominal dimension $0.25 \times 0.25 \times 0.5$ in. The surfaces to which the test load was applied were polished to a mirror-like finish.

Mechanical Testing

All tests were run on an Instron Floor Model TT-D. Uniaxial tensile tests were run on the previously described samples with a cross-head down speed of 0.002 in./min. All experiments were pursued until at least three load-deformation curves were obtained where the load passed through a maximum. (Since polystyrene is brittle in tension under ambient conditions, this load maximum could only be achieved with the slow testing rates and the specimen surface treatment described earlier.) Uniaxial compression tests were run on the previously described tetragonal specimens with the load applied parallel to the long dimension. The Instron compression plates were lubricated, and sample buckling was not noted until extensive strain beyond the maximum load occurred. Two different cross-head speeds were employed, one specimen run at 0.002 in./min and four specimens run at 0.02 in./min for each polystyrene of differing \bar{M}_n or MWD.

Data Treatment

This study had two primary sources of quantitative data—from GPC characterization and Instron operations. The GPC data were all handled in standard ways.¹⁵ However, the treatment of mechanical testing data can have many variations, and thus an account is presented here to give specific details of the procedure employed.

The Instron was operated such that the experimental variables were force,

cross-head travel rate, and sample dimensions. Thus, nominal strain was calculated by relating beginning sample length between the jaws and cross-head travel. Stress calculations were based on the observed force and cross-sectional area, where it was assumed that cross-sectional area changes were reliably determined as though constant volume deformation were occurring. Calculations to test this assumption showed that for the extent of deformation involved in this study, the stress so determined is essentially true stress.

The basic output from the Instron was recorded as a load-versus-deformation curve. Mechanical quantities such as modulus, proportional limit, and stress at the maximum load were obtained from this and the appropriate sample dimensions (see Tables II-IV).

Special emphasis was placed on characterizing the behavior of the samples in the region between the proportional limit and the maximum load. The nonlinear behavior of this region was curve fitted in the power law expression

$$\sigma = K\epsilon^n \quad (1)$$

This treatment provided quantitative accessibility to the experimentally generated stress-strain relationship (see Tables V-VII).

The point of using this treatment of stress-strain data is to enable the following. The behavior of polystyrene as represented by the above equation and its parameters could now be correlated by statistical linear regression analysis to MW and MWD. Thus, in the linear and beginning region of nonlinear behavior these results aid in building insight into the interactive roles of the mechanics and the molecular weight characteristics in the deformation process.

Mechanical Property-Molecular Weight Correlation Equations

From the data in Tables I-VII a set of correlation equations were generated that are descriptive of the deformation behavior of amorphous polystyrene. Where no significant trends occurred, the property was calculated using the values $\bar{M}_n = 650,000$ g/mole, or MWD = 2.00. Both of these represent "average" values, being in the approximate centers of the ranges of the investigation.

Initial Modulus. In all cases,

$$\text{initial modulus} = (3.55 \pm 0.06) \times 10^5 \text{ psi} \quad (2)$$

Stress (σ_p)

$$T(M) = (3.5 \pm 0.1) \times 10^3 \text{ psi} \quad (3)$$

$$T(D) = (3.93 \pm 0.15) \times 10^3 \text{ psi} - (299 \pm 68) \text{ (MWD) psi} \quad (4)$$

$$\begin{aligned} C(M) &= (5.5 \pm 0.4) \times 10^3 \text{ psi} \\ C(D) & \quad (5) \end{aligned}$$

Strain (ϵ_p)

$$T(M) = (0.96 \pm 0.03)\% \quad (6)$$

$$T(D) = (1.22 \pm 0.07) - (0.11 \pm 0.03) \text{ (MWD)\%} \quad (7)$$

$$\begin{aligned} C(M) &= (1.50 \pm 0.10)\% \\ C(D) & \quad (8) \end{aligned}$$

Power Law Equation ($\sigma = K\epsilon^n$)

TABLE II
Calculated Tensile Test Data

Polymer	Initial modulus, psi $\times 10^{-5}$	σ_p , psi $\times 10^{-3}$	ϵ_p , %	σ_m , psi $\times 10^{-3}$	ϵ_m , %
2	3.21	3.47	1.08	6.08	1.99
	3.11	3.70	1.19	6.25	2.18
	3.76	3.76	1.00	6.21	1.77
3	3.74	3.02	0.808	6.24	1.77
	3.89	3.65	0.939	6.25	1.91
	3.49	3.16	0.905	6.32	1.91
	3.29	3.32	1.01	6.31	2.06
4	3.60	2.97	0.826	6.30	1.91
	3.49	2.87	0.822	6.36	1.95
	3.35	3.72	1.11	6.38	2.05
	3.75	3.40	0.906	6.30	1.80
5	3.64	3.47	0.954	6.25	1.92
	3.77	3.53	0.937	6.34	1.81
	3.40	3.65	1.08	6.19	1.92
	3.57	3.57	1.00	6.16	1.82
6	3.74	3.64	0.973	6.57	1.86
	3.79	3.83	1.01	6.65	1.88
	3.59	3.43	0.956	6.56	2.05
	3.72	3.57	0.960	6.66	1.92
7	3.74	3.63	0.970	6.70	1.94
	3.66	3.54	0.967	6.60	1.91
	3.79	3.45	0.910	6.43	1.78
8	3.33	3.43	1.03	6.68	2.14
	3.75	3.33	0.887	6.50	1.80
	3.54	3.54	1.00	6.71	1.99
9	3.16	3.08	0.976	6.04	2.06
	3.26	3.06	1.00	6.08	2.96
	3.32	3.05	0.918	6.01	2.02
10	3.66	3.21	0.878	5.97	1.72
	3.68	3.06	0.832	6.00	1.75
	3.24	3.11	0.960	6.19	2.00
Bimodal mixture	3.26	3.42	1.05	6.24	2.09
	3.35	3.05	0.911	6.30	2.04
	3.43	3.27	0.954	6.21	1.96
Tetramodal mixture	3.27	3.40	1.04	6.23	2.03
	3.33	3.36	1.01	6.24	2.06
	3.36	3.36	1.00	6.18	1.97

TABLE III
 Calculated Compressive Test Data^a

Polymer	Initial modulus, psi $\times 10^{-5}$	σ_p , psi $\times 10^{-3}$	ϵ_p , %	σ_m , psi $\times 10^{-3}$	ϵ_m , %
2	3.69	5.02	1.36	11.8	4.72
3	3.69	5.28	1.43	11.8	4.75
4	3.55	5.61	1.58	11.3	4.98
5	3.64	5.20	1.43	11.6	4.85
6	3.38	6.43	1.90	11.5	4.83
7	3.57	5.67	1.59	11.5	4.76
8	3.63	5.45	1.50	11.4	4.89
9	3.70	5.96	1.61	11.9	4.75
10	3.78	5.40	1.43	12.0	4.77
Bimodal mixture	3.52	5.42	1.54	11.5	4.93
Tetramodal mixture	3.53	5.58	1.58	11.5	4.89

^a Cross-head down speed = 0.002 in./min.

$$T(M) \sigma = (3.55 \pm 0.25) \times 10^3 \text{ psi } (\epsilon^n) \quad (9)$$

where $n = (0.904 \pm 0.006) + (0.0027 \pm 0.0010)(\bar{M}_n \times 10^{-5})$.

$$T(D) \sigma = (3.55 \pm 0.25) \times 10^3 \text{ psi } (\epsilon^n) \quad (10)$$

where $n = (0.871 \pm 0.023) + (0.023 \pm 0.010)(MWD)$.

$$\begin{aligned} C(M) \\ C(D) \end{aligned} \sigma = (4.57 \pm 0.22) \times 10^3 \text{ psi } (\epsilon^{0.67 \pm 0.02}) \quad (11)$$

Stress (σ_m)

$$T(M) = (6.25 \pm 0.04) \times 10^3 \text{ psi} + (33 \pm 7)(\bar{M}_n \times 10^{-5}) \text{ psi} \quad (12)$$

$$T(D) = (6.25 \pm 0.09) \times 10^3 \text{ psi} - (74 \pm 39)(MWD) \text{ psi} \quad (13)$$

$$C(M) = (1.16 \pm 0.01) \times 10^4 \text{ psi} \quad (14)$$

$$C(D) = (1.17 \pm 0.02) \times 10^4 \text{ psi} + (187 \pm 77)(MWD) \text{ psi} \quad (15)$$

Strain (ϵ_m)

$$T(M) = (1.93 \pm 0.10)\% \quad (16)$$

$$T(D)$$

$$C(M) = (4.83 \pm 0.03)\% \quad (17)$$

$$C(D) = [(4.69 \pm 0.06) + (0.085 \pm 0.027)(MWD)]\% \quad (18)$$

DISCUSSION

The first trend considered is the importance of the strain regime to the influence of molecular weight parameters on mechanical properties. Note in the elastic region that modulus is independent of MW and MWD. However, as the strain level increases, correlations between mechanical properties and MW or MWD are established. Also, the intensity of the dependence seems to increase as the strain increases. Now this work is limited to the events happening from

TABLE IV
 Calculated Compressive Test Data^a

Polymer	Initial modulus, psi $\times 10^{-5}$	σ_p , psi $\times 10^{-3}$	ϵ_p , %	σ_m , psi $\times 10^{-3}$	ϵ_m , %
2	3.75	5.62	1.50	13.2	4.97
	3.77	6.25	1.66	13.0	4.89
	3.61	6.67	1.85	12.7	5.07
	3.71	5.90	1.59	13.0	5.08
3	3.69	5.76	1.56	13.1	5.22
	3.85	6.16	1.60	13.2	5.11
	3.80	6.61	1.74	13.0	5.15
	3.83	5.79	1.51	13.2	5.09
4	3.51	5.51	1.57	12.7	4.94
	3.76	6.84	1.82	12.8	5.02
	3.64	6.08	1.67	13.0	5.08
	3.72	5.35	1.44	12.9	5.03
5	3.81	6.33	1.66	13.1	5.13
	3.69	5.86	1.59	13.0	5.18
	3.75	5.73	1.53	13.0	5.21
	3.68	6.19	1.68	13.2	5.27
6	3.65	5.81	1.59	12.9	5.00
	3.73	6.53	1.75	12.9	5.00
	3.70	6.25	1.69	13.0	5.06
	3.67	5.69	1.55	12.5	5.13
7	3.59	5.67	1.58	12.6	5.14
	3.60	6.30	1.75	12.9	5.08
	3.83	6.40	1.67	13.1	5.08
	3.72	5.32	1.43	13.1	5.17
8	3.69	7.02	1.90	13.0	4.98
	3.77	6.90	1.83	12.9	5.02
	3.86	5.21	1.35	12.9	5.00
	3.88	5.74	1.48	13.2	5.06
9	3.72	5.40	1.45	13.0	5.02
	3.70	5.18	1.40	12.9	5.13
	3.59	5.57	1.55	12.8	5.18
	3.67	6.49	1.77	13.1	5.16
10	3.74	6.80	1.82	13.5	5.14
	3.74	6.80	1.82	13.2	5.14
	3.84	5.42	1.41	13.3	5.10
	3.77	6.86	1.82	13.4	5.23
Bimodal mixture	3.71	5.60	1.51	12.8	5.11
	3.41	5.70	1.67	12.9	5.44
	3.90	4.72	1.21	12.9	4.99
	3.73	6.46	1.73	13.0	5.27
Tetramodal mixture	3.57	5.43	1.52	12.8	5.03
	3.77	6.71	1.78	13.0	5.02
	3.69	5.80	1.57	12.8	5.11
	3.83	5.70	1.49	13.1	5.14

^a Cross-head down speed = 0.02 in./min.

TABLE V
Slope and Intercept of Log (True Stress) Versus Log (Nominal Strain) Plots for Tensile Tests

Polymer	Intercept K	Slope n	Correlation coefficient	Standard error, Y on X
2	3.515 ± 0.003	0.920 ± 0.014	0.999	0.0027
	3.508 ± 0.006	0.890 ± 0.025	0.995	0.0062
	3.578 ± 0.003	0.897 ± 0.016	0.998	0.0037
3	3.572 ± 0.002	0.933 ± 0.013	0.998	0.0047
	3.547 ± 0.002	0.918 ± 0.014	0.998	0.0042
	3.544 ± 0.002	0.939 ± 0.010	0.999	0.0035
	3.521 ± 0.003	0.920 ± 0.014	0.998	0.0042
4	3.555 ± 0.002	0.919 ± 0.014	0.998	0.0056
	3.544 ± 0.002	0.935 ± 0.012	0.998	0.0049
	3.531 ± 0.003	0.889 ± 0.012	0.999	0.0033
	3.576 ± 0.002	0.903 ± 0.014	0.998	0.0041
5	3.561 ± 0.004	0.869 ± 0.024	0.993	0.0076
	3.578 ± 0.002	0.892 ± 0.013	0.998	0.0037
	3.538 ± 0.004	0.929 ± 0.019	0.997	0.0049
	3.558 ± 0.003	0.923 ± 0.017	0.998	0.0043
6	3.576 ± 0.002	0.927 ± 0.012	0.999	0.0033
	3.585 ± 0.002	0.888 ± 0.011	0.999	0.0030
	3.561 ± 0.005	0.883 ± 0.024	0.993	0.0085
	3.574 ± 0.003	0.908 ± 0.014	0.998	0.0044
7	3.577 ± 0.003	0.906 ± 0.017	0.997	0.0053
	3.567 ± 0.002	0.929 ± 0.013	0.998	0.0039
	3.580 ± 0.003	0.942 ± 0.010	0.999	0.0030
8	3.525 ± 0.003	0.931 ± 0.012	0.999	0.0040
	3.576 ± 0.002	0.955 ± 0.012	0.999	0.0037
	3.551 ± 0.003	0.952 ± 0.013	0.998	0.0040
9	3.506 ± 0.004	0.912 ± 0.020	0.997	0.0062
	3.517 ± 0.003	0.943 ± 0.014	0.998	0.0043
	3.524 ± 0.003	0.879 ± 0.016	0.997	0.0060
10	3.558 ± 0.004	0.954 ± 0.026	0.995	0.0072
	3.564 ± 0.002	0.930 ± 0.016	0.998	0.0051
	3.514 ± 0.002	0.958 ± 0.012	0.999	0.0038
Bimodal mixture	3.520 ± 0.005	0.912 ± 0.025	0.994	0.0076
	3.528 ± 0.003	0.923 ± 0.016	0.997	0.0060
	3.538 ± 0.003	0.913 ± 0.016	0.997	0.0051
Tetramodal mixture	3.521 ± 0.004	0.924 ± 0.019	0.996	0.0057
	3.533 ± 0.006	0.873 ± 0.030	0.990	0.0058
	3.531 ± 0.004	0.922 ± 0.019	0.997	0.0055

TABLE VI
Slope and Intercept of Log (True Stress) Versus Log (Nominal Strain) Plots for Compressive Tests^a

Polymer	Intercept K	Slope n	Correlation coefficient	Standard error, Y on X
2	3.641 ± 0.018	0.700 ± 0.036	0.966	0.0228
3	3.653 ± 0.018	0.678 ± 0.037	0.964	0.0223
4	3.661 ± 0.020	0.623 ± 0.038	0.953	0.0221
5	3.646 ± 0.018	0.673 ± 0.037	0.962	0.0226
6	3.658 ± 0.021	0.640 ± 0.041	0.956	0.0183
7	3.654 ± 0.019	0.654 ± 0.038	0.961	0.0204
8	3.661 ± 0.019	0.639 ± 0.038	0.955	0.0228
9	3.668 ± 0.018	0.657 ± 0.036	0.965	0.0191
10	3.664 ± 0.019	0.672 ± 0.038	0.960	0.0233
Biomodal mixture	3.648 ± 0.019	0.654 ± 0.038	0.958	0.0225
Tetramodal mixture	3.655 ± 0.019	0.645 ± 0.038	0.957	0.0219

^a Cross-head down speed = 0.002 in./min.

zero strain up into the yield region. However, an extrapolation of these results in stress fields where fracture does not interfere suggests that the post yield region would manifest molecular weight effects to a greater extent than noted here.

The next consideration deals with the range of molecular weights under investigation. An important distinction must be made, that is, whether the \bar{M}_n of the polymer is above or below $2M_e$. Below $2M_e$ the tensile and perhaps other properties are extremely dependent on \bar{M}_n . One understands this from the view that at less than $2M_e$ the formation of a physically entangled network of chains is not complete.⁸ This leads to structural flaws of a serious nature which sharply influence mechanical properties and limit experimental study to the elastic region. Note in the present study all polystyrenes used were significantly above $2M_e$ ($2M_e$ of PS $\approx 70,000$). This is because we chose to emphasize the study of molecular weight effects in the yield region.

The spatial characteristics of the deformation mechanics are also of interest and bear a special relationship to the molecular weight parameters. To aid in the exposition of this relationship, two experimental observations are called to attention. Firstly, all mechanical property values except modulus are greatly different in tension versus compression. Secondly, while correlations between mechanical properties and molecular weight parameters are found for both tension and compression, the correlations are not the same. These observations suggest that the simultaneous scrutiny of the mechanics and structure in the molecular weight domain used here will be fruitful.

The cogent feature to consider comes from thinking about the strain fields associated with tension and compression. Generally, for deformation occurring only along the principal axes, one may write

$$\epsilon_{ij} = \begin{vmatrix} \epsilon_{11} & 0 & 0 \\ 0 & \epsilon_{22} & 0 \\ 0 & 0 & \epsilon_{33} \end{vmatrix}$$

TABLE VII
Slope and Intercept of Log (True Stress) Versus Log (Nominal Strain) Plots for Compressive Tests^a

Polymer	Intercept K	Slope n	Correlation coefficient	Standard error, Y on X
2	3.649 ± 0.018	0.736 ± 0.035	0.971	0.0212
	3.674 ± 0.019	0.693 ± 0.037	0.967	0.0195
	3.678 ± 0.020	0.654 ± 0.038	0.960	0.0190
	3.662 ± 0.019	0.698 ± 0.038	0.964	0.0219
3	3.662 ± 0.019	0.697 ± 0.036	0.964	0.0225
	3.684 ± 0.019	0.677 ± 0.036	0.964	0.0211
	3.695 ± 0.020	0.644 ± 0.037	0.959	0.0201
	3.674 ± 0.018	0.692 ± 0.035	0.966	0.0219
4	3.628 ± 0.018	0.739 ± 0.035	0.971	0.0203
	3.700 ± 0.019	0.631 ± 0.037	0.958	0.0188
	3.660 ± 0.019	0.700 ± 0.037	0.965	0.0208
	3.652 ± 0.018	0.715 ± 0.036	0.967	0.0231
5	3.686 ± 0.018	0.665 ± 0.035	0.065	0.0199
	3.659 ± 0.017	0.701 ± 0.032	0.965	0.0196
	3.671 ± 0.018	0.677 ± 0.035	0.961	0.0229
	3.678 ± 0.020	0.668 ± 0.037	0.960	0.0218
6	3.649 ± 0.019	0.720 ± 0.037	0.967	0.0212
	3.680 ± 0.019	0.668 ± 0.036	0.966	0.0185
	3.675 ± 0.019	0.673 ± 0.037	0.963	0.0205
	3.661 ± 0.019	0.677 ± 0.036	0.961	0.0224
7	3.652 ± 0.019	0.690 ± 0.037	0.962	0.0225
	3.667 ± 0.020	0.677 ± 0.037	0.962	0.0203
	3.690 ± 0.019	0.660 ± 0.037	0.962	0.0206
	3.652 ± 0.019	0.719 ± 0.037	0.964	0.0245
8	3.694 ± 0.020	0.647 ± 0.038	0.961	0.0180
	3.696 ± 0.020	0.646 ± 0.039	0.959	0.0191
	3.660 ± 0.017	0.711 ± 0.034	0.968	0.0232
	3.676 ± 0.019	0.694 ± 0.037	0.963	0.0232
9	3.651 ± 0.017	0.724 ± 0.035	0.969	0.0221
	3.651 ± 0.017	0.714 ± 0.034	0.967	0.0235
	3.646 ± 0.019	0.707 ± 0.036	0.964	0.0226
	0.675 ± 0.020	0.676 ± 0.037	0.963	0.0198
10	3.687 ± 0.020	0.675 ± 0.037	0.963	0.0195
	3.692 ± 0.020	0.656 ± 0.037	0.961	0.0195
	3.661 ± 0.018	0.721 ± 0.035	0.968	0.0232
	3.697 ± 0.021	0.654 ± 0.039	0.956	0.0207
Bimodal mixture	3.659 ± 0.018	0.696 ± 0.036	0.966	0.0220
	3.635 ± 0.020	0.701 ± 0.036	0.965	0.0220
	3.653 ± 0.015	0.730 ± 0.032	0.969	0.0247
	3.692 ± 0.021	0.641 ± 0.038	0.956	0.0215
Tetramodal mixture	3.638 ± 0.019	0.730 ± 0.037	0.968	0.0221
	3.697 ± 0.019	0.642 ± 0.035	0.963	0.0185
	3.663 ± 0.019	0.685 ± 0.036	0.964	0.0218
	3.670 ± 0.018	0.690 ± 0.036	0.967	0.0220

^a Cross-head down speed = 0.02 in./min.

More specifically, for the uniaxial case one writes for constant volume deformation

$$\epsilon_{ij} = \begin{vmatrix} \epsilon_{11} & 0 & 0 \\ 0 & \frac{-\epsilon_{11}}{2} & 0 \\ 0 & 0 & -\frac{\epsilon_{11}}{2} \end{vmatrix}$$

where $\epsilon_{11} = \partial u_1 / \partial x_1$, and $\epsilon_{11} > 0$ for tension and $\epsilon_{11} < 0$ for compression. In uniaxial tension the positive strain is one-dimensional, and so is the major molecular transport occurring to accommodate the mechanical forces placed on the sample. In compression, however, the positive strain is biaxial, and so is the molecular transport. The molecular response of a polymer in uniaxial tension is fundamentally different from that in uniaxial compression!

This can be more fully appreciated by thinking in terms of the physically entangled chain model. First, consider a single entanglement in uniaxial tension. It can respond in the load bearing sense by reacting to a force with a single direction. Just prior to molecular fracture, then, a unique combination of force and entanglement position exists. On the other hand, think in terms of a single entanglement in biaxial tension. Here, a range of positions exist for the entanglement just prior to molecular fracture. (Figure 1 attempts to graphically represent this situation.) This would be in analogy to a system with one degree of freedom versus another system with two degrees of freedom.

One can imagine that in uniaxial tension a time- and temperature-dependent "limit" is reached where an entanglement cannot accommodate further stress by any further molecular relaxation. Consequently, an increased stress produces fracture. This line of reasoning is in complete accord with the theory of finite tensile rubber extensibility for chemically crosslinked elastomers. Now in the case of biaxial deformation the role of the physical entanglement is significantly different. Instead of the entanglement being restricted by a one-dimensional space-mechanical force relation, a range of responses is available. This leads to a multiplicity of positions and thus movement on the molecular chain segment level. This movement or "yielding" would certainly come at a higher stress level as observed, but yet its occurrence is still possible. Thus, biaxial response of a polymeric material produces a viable alternative to molecular rupture.

The above interpretation is validated by a further experimental reality. The exponent n in the power law expression, eq. (1), is lower valued in compression than in tension. An n value of 1 is, of course, characteristically "elastic." As n decreases, "plastic" behavior is more and more favored. Also, while this plastic behavior is favored, it occurs at a higher stress in agreement with the above thinking of chain segmental movement in a biaxial stress field.

The foregoing view of the mechanism of deformation is compatible with the phenomenological behavior of biaxially oriented polystyrene reported by Cleereman.¹⁶ One can speculate from the above mechanism that the interacting roles of the deformation mechanics and molecular weight parameters can be advantageously employed. It should be possible with the proper combination of applied stress field, chain entanglement structure, and chain orientation to result in the specimen undergoing the yielding phenomenon and subsequent plastic deformation at high stress levels.

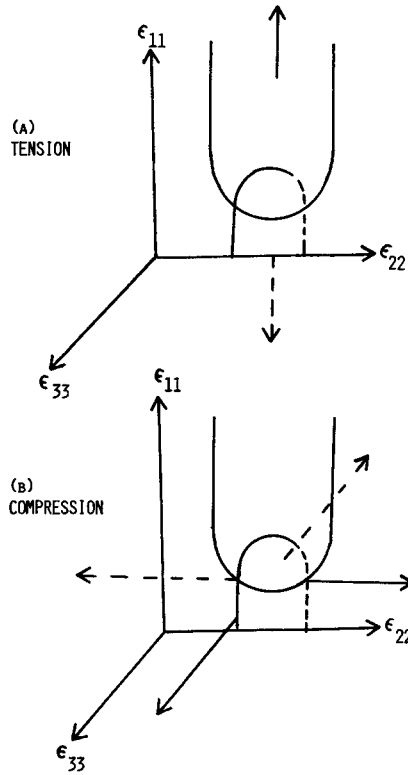


Fig. 1. Graphic representation of a chain entanglement (a) in uniaxial tension and (b) in uniaxial compression.

List of Symbols Employed

\overline{MW} molecular weight

\overline{M}_w weight-average molecular weight

\overline{M}_n number average molecular weight

MWD molecular weight distribution

M_e molecular weight between entanglements

σ stress

σ_m stress calculated at maximum load

σ_p stress at the onset on nonlinear behavior

ϵ strain

ϵ_m strain corresponding to σ_m

ϵ_p strain corresponding to σ_p

ϵ_{ij} second order strain tensor

K proportionality constant for power law equation

n exponent on power law expression reflecting sample deformation resistance in nonlinear region

PS polystyrene

PMMA poly(methyl methacrylate)

PC polycarbonate

T temperature

T_g glass transition temperature

GPC gel permeation chromatography
T(M) tensile property versus \bar{M}_n
T(D) tensile property versus MWD
C(M) compressive property versus \bar{M}_n
C(D) compressive property versus MWD

The authors are pleased to acknowledge the partial support of this project through a grant from the National Science Foundation, DMR 75-02958. They are also happy to express their gratitude to Professor J. E. Spruiell for his enlightening discussions of the phenomenological characterization of stress-strain behavior.

References

1. S. S. Sternstein, L. Ongchin, and A. Silvermann, *Appl. Polym. Symp.*, **7**, 175 (1968).
2. L. C. Cessna, Jr., and S. S. Sternstein, *Fundamental Phenomena in Materials Sciences*, Plenum Press, New York, **4**, 45 (1967).
3. P. Bowden and S. Raha, *Philos. Mag.*, **22**, 463 (1970).
4. G. Langford, W. Whitney, and R. D. Andrews, Mater. Res. Lab. Res. Rept. No. R63-49, MIT School of Engineering, Cambridge, Mass., 1963.
5. W. Whitney and R. D. Andrews, *J. Polym. Sci.*, **C16**, 2981 (1967).
6. J. R. Martin, J. F. Johnson, and A. R. Cooper, *J. Macromol. Sci.—Rev. Macromol. Chem.*, **C8(1)**, 57 (1972).
7. S. L. Kim, M. Skibo, J. A. Manson, and R. W. Hertzberg, *Polym. Prepr.*, **16(2)**, 559 (1975).
8. J. F. Fellers and B. F. Kee, *J. Appl. Polym. Sci.*, **18**, 2355 (1974).
9. S. S. Sternstein and L. Ongchin, *Polym. Prepr.*, **10(2)**, 1117 (1969).
10. K. Matsushige, S. V. Radcliffe, and E. Baer, *J. Mater. Sci.*, **10**, 833 (1975).
11. K. Matsushige, S. V. Radcliffe, and E. Baer, *J. Polym. Sci., Phys. Ed.*, **14**, 703 (1976).
12. A. N. Gent, *J. Mater. Sci.*, **5**, 925 (1970).
13. A. N. Gent and G. Thomas, *J. Polym. Sci. A-2*, **10**, 571 (1972).
14. H. W. McCormick, F. M. Brower, and L. Kin, *J. Polym. Sci.*, **39**, 87 (1959).
15. J. Cazes, *J. Chem. Educ.*, **47**, A561 and A505 (1970).
16. K. J. Cleereman, *Polym. Prepr.*, **14(1)**, 256 (1973); *Appl. Polym. Symp. No. 24*, 31 (1974).

Received March 8, 1977

Revised April 12, 1977